Compositional distribution in the first monolayers from evaluation of XPS and AES spectra

Wolfgang S.M.Werner

Institut für Angewandte und Technische Physik,
Vienna University of Technology, Wiedner Hauptstr. 8–10
1040 Vienna, Austria
e-mail:werner@iap.tuwien.ac.at

(Received: Jan. 31, 1997 Accepted: Feb. 21, 1997)

Abstract

Non destructive nanoanalysis of the outermost atomic layers of a solid plays an increasingly important role in materials characterization. Owing to their high surface sensitivity, the electron spectroscopic techniques AES and XPS can be used for this purpose via analysis of the energy and angular shape of the emitted signal electron distribution. One method to achieve this goal, the so-called partial intensity analysis, seems particulary promising since it allows to properly account for a vast majority of phenomena affecting the signal electron excitation and escape process in a straightforward way. In particular, it accurately describes the energy dependence of the electron solid interaction. Thus it can not only be used to analyze the spectral shape of Auger and photoelectron lines but also the broad background of backreflected primaries in electron excited AES. This opens up a way for true 3-dimensional nondestructive nanoanalysis on the basis of scanning Auger experiments.

1. Introduction

The development of any measurable physical process into a routine analysis procedure usually proceeds in three steps: (1.) theoretical modelling of the basic physical process; (2.) determination of the fundamental parameters entering this model; and (3.) deriving a procedure to extract the desired information from the quantities assessable to experiment. The past decade has seen a wealth of developments for surface analysis by electron spectroscopy in all of the above three fields.

Accurate theoretical models have been devised for the angular and energy distribution of signal electrons in AES/XPS. The probably most extensively studied phenomenon is the influence of elastic scattering on the signal electron yield [1-4], but accurate models have also been developed for the influence of phenomena like surface roughness [5,6], surface excitations [7,8], the experimental geometry and asymetric photoelectron emission [9,10], depth [11] and energy [12] dependence of the scattering characteristics, etc.

Although many of the physical parameters relevant for AES/XPS can be calculated ab initio this is not generally possible for the most important one that quantitatively determines the surface sensitivity of these techniques: the inelastic mean free path (IMFP). Consequently, a vast number of theoretical [13-15] and experimental [16-18] works has been devoted to the study of this quantity. Also, absolute sensitivity factors have been established for a large number of elemental solids and compounds [19-22].

Several procedures for quantitative spectral interpretation have been proposed and are constantly being refined. Among them we note methods for inelastic background subtraction [2,4,23-26], various quantification schemes for homogeneous solids [27], angle resolved AES and XPS [28-30] and inelastic background analysis [31-33] for compositional depth profile determination and, recently, the so–called partial intensity analysis [11] allowing to extract information on the compositional distribution from evaluation of the entire energy and angular distribution of signal electrons in AES/XPS.

At this stage it is advisable to consider an important question for practical applications: to what extent are the spectrum interpretation methods able to account for the developments in the accurate theoretical modelling of the spectra? Obviously, it would be highly desirable for a spectrum processing technique to be able to account precisely for the physics of the signal electron generation process since otherwise the usefullnes of further developing the theory of the basic processes would be purely academic.

A very general quantitative spectrum interpretation method that is able to account for the details of the signal electron generation is the so–called partial intensity analysis [11]. It allows to extract structural information from the availiable experimental data on the angular and energy distribution of signal electrons and even the most sophisticated model for the signal electron generation can be incorporated in this method in a straightforward way. Since the surface sensitivity of AES/XPS is very high, this allows to perform nano–depth profiling.
In the next sections we will outline the theoretical description of the spectral yield based on the partial intensity formalism and derive the procedure to invert a measured spectrum into structural information, the so–called partial intensity analysis. Finally, the basic ideas will be illustrated with some applications.

2. Partial Intensity Formalism for the Spectral Intensity

In non–crystalline solids, the transfer of signal electrons is governed by a Boltzmann type kinetic equation [34]. This implies [12] that the stochastic process for multiple scattering obeys the Poisson distribution. In other words, the probability for an electron to experience an energy loss increases with the path length travelled in the solid. Consider e.g. Auger electron emission from an elemental solid. Let us suppose, for a moment, that the distribution of path lengths travelled by the signal electrons is known and is given by $Q(s,\Omega)$, where s denotes the path length and Ω is the emission direction. Then the number of electrons $y(E,\Omega)$ emitted into this direction with a certain energy E is obtained by multiplying the path length distribution with the probability that the electron flux density has a certain energy distribution after travelling a given path length and integrating over all possible path lengths:

$$y(E,\Omega) = \int Q(s,\Omega)\ F(s,E)\ ds \qquad (1)$$

The energy distribution after travelling the path length s, F(s,E) is obtained by multiplying the intrinsic spectrum f(E) with Landau's energy loss function G(s,E-E') and integrating:

$$F(s,E) = \int f(E')\ G(s,E-E')\ dE' \qquad (2)$$

Equation (1) and (2) completely specify the solution of the transport problem as they represent a rigorous solution of the kinetic equation [2].
There exists an alternative and sometimes more convenient method to describe the spectrum. It is based on the observation that, according to Poisson statistics, the number of inelastic collisions n increases with the path length, or, in other words, the number of inelastic collisions may alternatively be used to keep track of the particle's energy. The number of electrons $C_n(\Omega)$ that escape after n collisions is found by multiplying the path length distribution with the probability $W_n(s)$ for n losses after travelling a given path length and integrating:

$$C_n(\Omega) = \int Q(s,\Omega) W_n(s) ds \qquad (3)$$

The probability for a given energy loss ε=E-E' in an individual inelastic collision is described by the differential inelastic inverse mean free path $w(\varepsilon)$ (DIIMFP, sometimes called inelastic cross section). This quantity can be obtained from dielectric response theory using optical data [15] or alternatively, Tougaards universal cross section may be used in some cases [35].
Let us suppose that we know the energy distribution $F_n(E)$ after n losses. Then the energy distribution after n+1 losses is obtained by multiplying with the probability for an individual loss w(E-E') and integrating over all energy losses:

$$F_{n+1}(E) = \int w(E-E')\ F_n(E')\ dE' \qquad (4)$$

and

$$F_0(E) = f(E) \qquad (5)$$

Thus, the partial energy distributions $F_n(E)$ can simply be calculated as an n–fold convolution of the intrinsic spectrum with the single scattering loss probability $w(\varepsilon)$.
Obviously, a spectrum $y(E,\Omega)$ comprises contributions of electrons having experienced a different number n inelastic processes. The (normalized) energy distribution of the n–th group is given by Eq.(4). The number of electrons in the n–th group is just equal to the n–th partial intensity. Therefore the spectrum is obtained by summing up the contributions of all groups:

$$y(E,\Omega) = \sum_{n=0}^{\infty} C_n(\Omega) F_n(E) \qquad (6)$$

It should be emphasized at this stage that we have derived, with a simple physical argument, two equivalent formulations of the energy and angular distribution of signal electrons (Eq.(1) and (6)). It can be rigorously shown that these equations are the formal solution of the kinetic equation [2]. The reason why one may choose the independent variable keeping track of the particle energy (a discrete variable n or a continuous variable s) is related to the fact that the kinetic equation does not explicitly depend on the energy, as was already pointed out by Landau [36]. Landau's solution of the transport problem Eq. (1) has been used by most authors to tackle the transport problem in electron spectroscopy while the partial intensity formalism was only recently introduced in this connection by the present author. For several reasons, it is sometimes preferable to use the partial intensity approach.

First of all, it should be noted that both Eq. (1) and (6) are only formal solutions and to actually calculate the spectrum one needs to determine the path length distribution or the partial intensities for the structure under consideration. In doing so, one has to accurately account for the depth profile of the analyte as well as the variety of phenomena influencing the spectrum as mentioned in the introduction. To calculate the path length distribution for such a situation is a tedious task that can only be performed numerically except for the most simple but physically not very realistic models. The partial intensities on the other hand can simply be calculated for an arbitrary depth profile c(z) using the relationship [11]:

$$C_n(\Omega) = \int c(z) \; P_n(z,\Omega) \; dz \qquad (7)$$

where $P_n(z,\Omega)$ are the so-called partial escape distributions. Analytic expressions for these quantities have been recently derived that account for elastic scattering [33], surface roughness [6], asymmetry of photoelectron emission [9], etc. Thus the first practical advantage of the partial intensity formalism is that the crucial quantities that depend on the compositional depth profile, the partial intensities, can be more easily determined than the path length distribution.

The second important practical point is that the partial intensities can be derived from an experimental spectrum. This, in fact, is the basis of the so-called partial intensity analysis to be discussed in the next section. This does not seem to be possible for the path length distribution. Only indirectly, by first determining the partial intensities and inverting Eq. (3) the path length distribution can be obtained.

Finally, extension of the partial intensity formalism beyond the quasi-elastic regime is straightforward while this is slightly more involved for the path length distribution approach. In the quasi-elastic regime, the energy loss is assumed to be small enough to neglect the change of e.g. the inelastic mean free path λ with the number of inelastic collisions, Hence the probability for n losses is given by the Poisson distribution:

$$W_n(s) = \frac{1}{n!}\left(\frac{s}{\lambda}\right)^n e^{-s/\lambda} \equiv P_n\left(\frac{s}{\lambda}\right) \qquad (8)$$

When the quasi-elastic approximation is no longer admissible, Eq. (8) should simply be replaced by [12]:

$$W_n(s) = W_n(s) = \frac{\lambda_n}{\Lambda_n} P_n\left(\frac{s}{\Lambda_n}\right) \qquad (9)$$

where λ_n is the mean free path after n collisions and Λ_n is the average mean free path after n collisions:

$$\Lambda_n = \sum_{k=0}^{n} \lambda_k \,/\, (n+1) \qquad (10)$$

In the quasi-elastic case the inelastic mean free path is assumed to be independent of n: $\lambda_n=\lambda_{n-1}=\lambda_{n-2}.....=\lambda$ and Eq. (9) is found to reduce to the Poisson distribution Eq. (8). For large losses, the correspondence between the partial intensity formalism and the continuous slowing down approximation may be seen by observing that:

$$(n+1)\Lambda_n = R \qquad (11)$$

where R is the linear range that plays the role of characteristic length in the continuous slowing down approximation. The rather extensive discussion of the partial intensity formalism to model large losses may seem a little out of context here since the AES/XPS peaks usually lie within the quasi-elastic regime. However, as will be seen below, it is important since the partial intensity formalism not only allows to model the peaks in an electron spectrum, but also the background of backscattered primaries and the backscattering factor in electron excited AES.

3. Partial Intensity Analysis for Nanostructure Determination.

In the previous section a rigorous description of the quantity assessable in an AES/XPS experiment have been given. It will be shown next how this description may be utilized to extract structural information from the energy and angular distribution via a so–called partial intensity analysis.

It can be seen from Eq.(6)–(8) that only the escape mechanism is influenced by the compositional depth profile. Therefore, if the loss mechanism is quantitatively understood, it would be convenient to transform the raw data in such a way that an equation for the partial intensities remains. Let us assume that the depth profile can be parameterized by the variables $X=(x_1,x_2,...)$. Then one can write $C_n=C_n(X)$. The core of the partial intensity analysis is determination of these quantities, either directly, or by first determining the profile X and using Eq.(7) to calculate the partial intensities. When reference spectra y_r with known partial intensities C_{nr} are available this can be achieved by solution of the following set of equations [11]

$$\sum_{n=0}^{N}\{Y_n(E)C_{nr} - Y_{nr}(E)C_n(X)\} = 0 \qquad (12)$$

where Y_n stands for the n–fold convolution of a given spectrum y(E) with the normalized DIIMFP:

$$Y_n(E) = y(E) \otimes L_n(E) \qquad (13)$$

Alternatively, one may use two (or more) spectra of the unknown sample acquired at different emission geometries. Then the corresponding equation for the partial intensities reads:

$$\sum_{n=0}^{N}\{Y_{n1}(E)C_{n2}(X) - Y_{n2}(E)C_{n1}(X)\} = 0 \qquad (14)$$

where the subscript 1 and 2 denote the emission geometry. Neither the true intrinsic spectrum f(E) nor the analyzer transmission function etc. is present in Eq. (12) and (14). This implies that none of these quantities need be known for the partial intensity analysis of non–overlapping peaks.

Note that in the theory section we have tacitly assumed that every electron that leaves the surface reaches the detector, i.e. it was assumed that the factors like the analyzer transmission and the excitation rate etc. are equal to unity. Generally, the theoretical spectra Eq. (2) and (6) should be multiplied by these factors. In the partial intensity analysis, these factors cancel out. If a partial intensity analysis is applied to several lines of the same sample, then of course relative intensities do enter the analysis [11]. It is also pointed out in this connection that Eq. (12) and (14) were derived for the typical AES geometry when the area of the sample seen by the analyzer is large compared to the analyzed area.

Thus, Eq. (12) or (14) allow to determine the partial intensities and the depth profile by using Eq. (7). It should be noted in this connection that the equations for the partial intensities Eq. (12) and (14) represent a (usually heavily) overdetermined system of linear equations. Therefore the numerically most straightforward and stable way to solve these equations is to parametrize the depth profile by a possibly small number of parameters and to minimize the functionals Eq. (12) or (14) and using Eq. (7) to relate the depth profile to the partial intensities [11].

The procedure outlined above thus represents a convenient way to determine the partial intensities and thereby extract information on the compositional depth profile. However, it does even more than that. Knowledge of the partial intensities also constitutes the basis for a rigorous background subtraction method for an arbitrary depth profile and emission mechanism. To appreciate this point, recall that the zero order partial intensity is equal to the peak intensity while the spectral intensity deposited in the inelastic tail corresponds to the higher order partial intensities. Thus the zero order partial intensity is equal to the peak area corrected for the inelastic tail and background correction is implicitly carried out in the course of a partial intensity analysis. Hence, the partial intensity analysis significantly differs from the conventional quantification schemes that require subtraction of the inelastic tail prior to application of some kind of quantification algorithm.

Sometimes the aim of the analysis is not only quantitation but in addition it is desirable to study the intrinsic lineshape. Such a lineshape analysis can be performed once the partial intensities are known by application of the deconvolution formula [9,11]:

$$f(E) = W_N(y(E)) \qquad (15)$$

where the operator W is defined recursively as:

$$W_n(f) = W_{n-1}(f) - q_n \int L_n(E - E')W_{n-1}(f(E'))dE' \quad (16)$$

here L_n are the partial loss distributions and the coefficients q_n are a function of the partial intensities [11]. For the special case of a homogeneous sample with isotropic source emission, Eq (15) and (16) reduce to the formula by Tilinin and Werner [2], that is very similar to Tougaard's earlier result but differs from the latter in that it accounts for the emission angle dependence. The advantage of Eq. (15) and (16) is that it is valid for an arbitrary emission mechanism since it holds for any sequence of partial intensities. Therefore it is very general and can account for all phenomena influencing the emission mechanism through the choice of the proper partial intensities.

4. Application of the Partial Intensity Formalism for the Spectral Yield.

Before we turn to illustrations of the yield formula Eq. (6) and the partial intensity analysis, it seems advisable to study some exemplary cases of the quantities entering these formalisms.

The partial escape distributions P_n for 1000 eV electrons in Silver are shown in Fig. 1. The solid lines correspond to the rectilinear motion model leading to Poisson–type partial escape distributions while the dashed lines were calculated by solving the Boltzmann equation accounting for elastic scattering using the transport approximation [17]. The area under these curves give the partial intensities for a homogeneous solid (cf. Eq. (7)). These curves are instructive in that they allow to deduce how the sequence of partial intensities depends on the depth profile. For example, if the analyte is present as a thin layer at the surface, say in the depth region $0 \leq z \leq \lambda_i$, the partial intensities decrease monotonically with n while for $2\lambda_i \leq z \leq 3\lambda_i$ there will be a maximum for n~2.

To see how a given sequence of partial intensities translates into the spectral shape, it is necessary to inspect the partial energy distributions F_n. These quantities are the convolution of the partial loss distributions L_n with the intrinsic spectrum f(E). The normalized loss distribution for a Tougaard–type DIIMFP is shown in Fig. 2 as a function of the reduced energy loss $\varepsilon/\underline{\varepsilon}$ where $\underline{\varepsilon}$ is the mean energy loss in an individual collision. (The zero order partial loss distribution is a delta function at ε=0 and is not shown.)

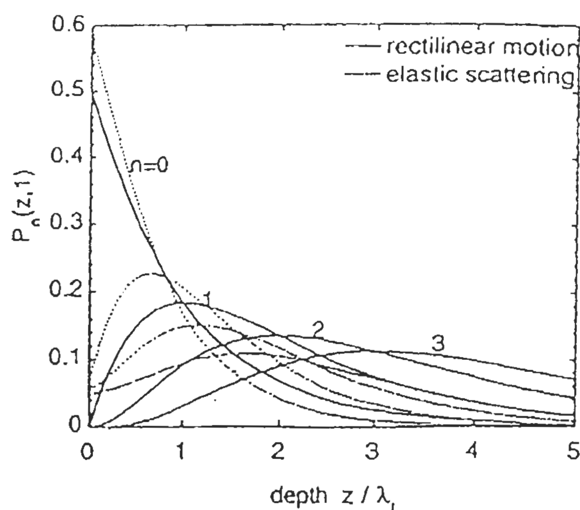

Fig. 1 Partial escape distributions P_n at normal emission for 1000 eV electrons emitted in a homogeneous Ag sample.

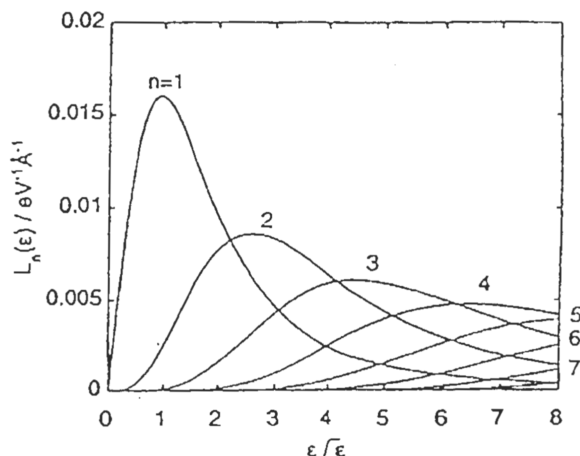

Fig. 2 Partial loss distributions L_n on the basis of a Tougaard type single scattering loss function (n=1).

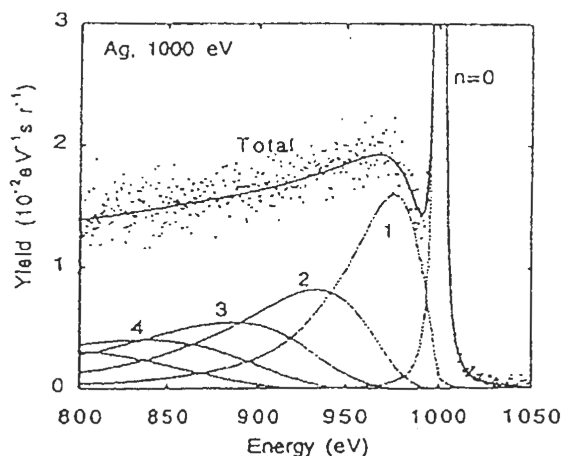

Fig. 3 Model spectrum calculated on the basis of the data presented in Fig. 1 and 2. (see text).

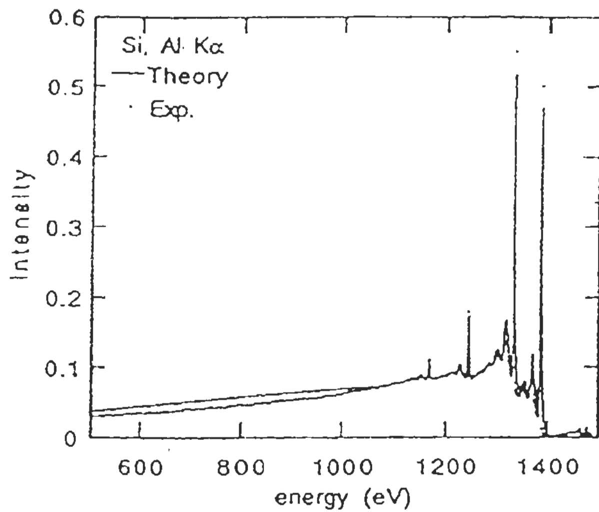

Fig. 4 Comparison of the partial intensity formalism for the photoelectron yield with experiment. Data points: experimental Si XPS spectrum acquired with Al Kα photons. Solid line: Eq. (6).

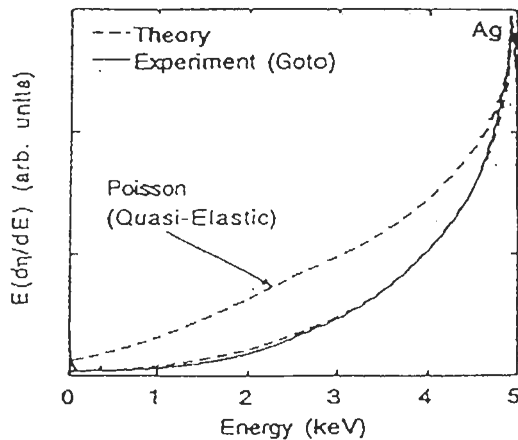

Fig. 5 Backscattering coefficient of 5 keV electrons normally incident on an Ag surface. Solid line: experimental results by Goto [37]. Dahsed line labelled "Poisson": theoretical result in the quasi-elastic approximation based on the Poisson stochastic process (Eq. (8)). Unlabelled dashed line: results of the partial intensitiy formalism using Eq. (9) for the multiple scattering stochastic process.

Performing the convolution of the intrinsic spectrum to obtain the partial energy distributions, weighting the latter quantities with the partial intensities and summing up the contributions for all n, the energy spectrum is obtained. This is illustrated in Fig. 3 for a Lorentzian intrinsic spectrum and a homogeneous Ag substrate using the partial intensities accounting for elastic scattering [2]. The thick solid line is the theoretical result, the data points are results of Monte Carlo calculations. The contribution of n–fold inelastically scattered particles is also shown as dashed lines. It may be emphasized again that the area under these curves corresponds to the partial intensities. For a homogeneous sample the partial intensities decrease monotonically with n: $C_n=\kappa^n$ ($\kappa<1$) [2] and consequently a decrease of the inelastic tail with energy loss can be observed. It is thus quite easy to conceive how the spectral shape changes with the depth profile on the basis of Fig. 1–3. In fact, the energy spectrum roughly follows the sequence of partial intensities and we conclude that these quantities are a fingerprint of the emission mechanism in the spectrum.

At this stage it is possible to examine the limit of the depth resolution of a depth profile determined with non–destructive electron spectroscopy. It is seen in Fig. 2 that the number of partial intensities depends on the width of the chosen energy window E_m: $n\sim E_m/\varepsilon$. Assuming that the rectilinear motion model holds, the mean depth of the Poisson type partial escape distribution is

$$\langle z\rangle_n = (n+1)\lambda_i \tag{17}$$

If the mean depth and width of the partial escape distributions may be taken for the mean depth and uncertainty of the depth from which n–fold inelastically scattered electrons originate, then the probing depth is given by $(E_m/\varepsilon+1)\lambda_i$. The relative error in the depth scale is found to be equal to $(n+1)^{-1/2}$, or, using Eq. (17) for the mean partial escape depth to eliminate the dependence on n, the relative depth resolution is found to be:

$$\frac{\Delta z}{z} \sim \frac{\sqrt{\langle z^2\rangle_n - \langle z\rangle_n^2}}{\langle z\rangle_n} = \frac{1}{\sqrt{n+1}} \sim \sqrt{\frac{\lambda_i}{z}} \tag{18}$$

These simple considerations demonstrate that the depth scale probed can be extended by enlarging the energy window at the price of a deterioration of the depth resolution. In particular, the absolute uncertainty in the depth is always larger than λ_i for depths larger than λ_i. For non–normal emission geometries λ_i should be replaced by $\lambda_i\cos\theta$ in the above.

A comparison of the partial intensity formalism with experimental data is shown in Fig. 4. The data points show an experimental Al Kα XPS spectrum of a pure Si sample sputter cleaned with Ar. The solid line represents the theoretical result. It is seen that all features of the spectrum like the relative intensity of the

peaks, the plasmon loss features as well as the inelastic tail are properly reproduced by theory. As an example of a situation where the energy dependence of the scattering characteristics is essential, Fig. 5 shows the differential backscattering coefficient of 5keV electrons normally incident on a Silver target. The solid line represents the experimental data by Goto [37], the dashed line labelled "Poisson" is the theoretical result in the quasi–elastic approximation using Eq. (8) to describe the stochastic process for multiple scattering. By merely using Eq. (9) instead of Eq (8) for the probability for n inelastic collisions in Eq. (3) the unlabelled dashed line is obtained as the result of the partial intensity formalism [12]. This approach is seen to compare excellently with experiment.

5. Application of Partial Intensity Analysis to Non–Destructive Nano-structure Determination.

In this section we will present a few illustrative examples of applications of partial intensity analysis to model spectra as well as real experimental data. Fig. 6 shows an application of the partial intensity analysis to model data. The intrinsic spectra shown in Fig. 6a were used to calculate the extrinsic spectra in Fig. 6b that correspond to the depth profile shown in the inset. The extrinsic spectra were calculated for two emission geometries (0° and 60° emission angle) for isotropic source emission [11]. These data were subjected to a partial intensity analysis. For overlapping peaks in the considered energy window, a modification of Eq. (14) has to be used. This is described in detail in Ref. [11]. Such an analysis leads to the partial intensities shown in Fig. 6c. The closed circles correspond to the reconstructed substrate partial intensities, the open circles are the overlayer partial intensities. The solid lines are the model values corresponding to the depth profile shown in Fig. 6b. Finally, the reconstructed depth profile is shown in Fig. 6d and compared with the original (model) depth profile. The agreement between the model and reconstructed depth profile is seen to be very good.

At this point it should be noted that the conventional evaluation algorithms based on only peak intensities merely consider the data points for n=0 in Fig. 6c and, so to speak, throw away the information contained in the higher order partial intensities. As can be seen in Fig.

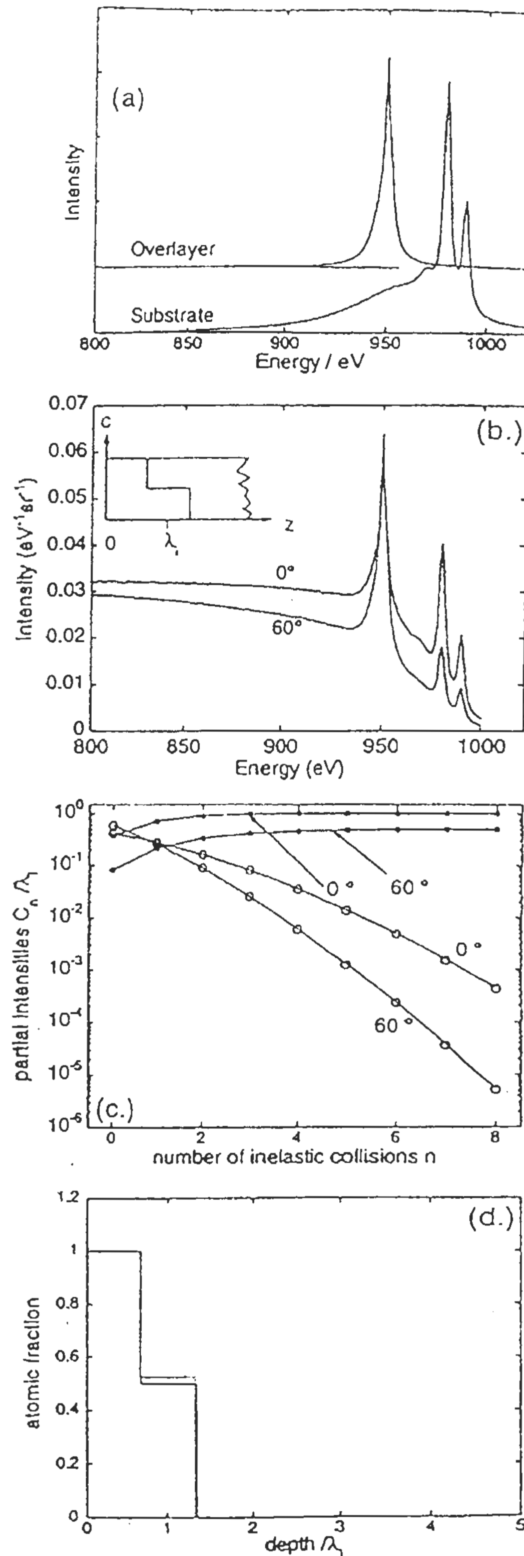

Fig. 6 Illustration of partial intensity analysis on model spectra. (a) Intrinsic model lineshapes for the overlayer and substrate material. (b) model spectra. The inset shows the model depth profile. (c) reconstructed partial intensities compared with model values. (d) reconstructed depth profiles compared with the model depth profile.

6c there is quite a large amount of information in the higher order partial intensities and consequently a consistent method like the partial intensity analysis that uses this information should prove useful in non-destructive nano-profiling.

An example of a partial intensity analysis of experimental Auger spectra of thin Au layers on a Pt substrate is shown in Fig. 7. These spectra were taken from a sample consisting of a ~80Å thick Au overlayer on a Pt substrate. The overlayer was removed by repeated cycles of Kr ion sputtering. The number of sputter cycles for each spectrum is indicated in the figure. The data points are the experimental Auger spectra after correcting for the inelastic background of backreflected primaries. The procedure to achieve this is described in Ref. [38]. The data displayed in Fig. 7 were corrected for the analyzer transmission function by means of the electron reflection method [39]. A partial intensity analysis was performed on these data prior to the analyzer transmission function correction, since the analyzer transmission function needs not be known for the partial intensity analysis. The depth profile was parametrized by a pure Au layer on top of a mixed layer containing both elements and a pure Pt substrate. Thus the thickness of the top layer as well as the concentration and thickness of the intermediate layers were used as unknowns. The analysis showed that the Au overlayer is homogeneous and no mixed layer does exist. Therefore the thickness of the overlayer is the only parameter remaining to be determined. These thicknesses are shown in Fig. 7b as a function of sputter time. Extrapolation of this curve to the thickness before sputtering leads to a thickness of 68Å which is in good agreement with the nominal value of 80Å.

After determination of the overlayer thickness, the theoretical spectra were calculated with Eq. (6). The spectra corresponding to the retrieved overlayer thicknesses are displayed as solid lines in Fig. 7 and are seen to match the experimental data quite well. The satisfactory agreement between the theoretical spectra and the experimental data corrected for the analyzer transmission indicates that the analyzer transmission correction was performed properly. It should again be emphasized that for the partial intensity analysis per se, such a correction of the spectra is not necessary. If one wishes to compare the theoretical spectra corresponding to the retrieved profile with the experimental data, then naturally, the latter need to be properly calibrated. Note that this constitutes an essential difference between the partial intensity analysis and other methods

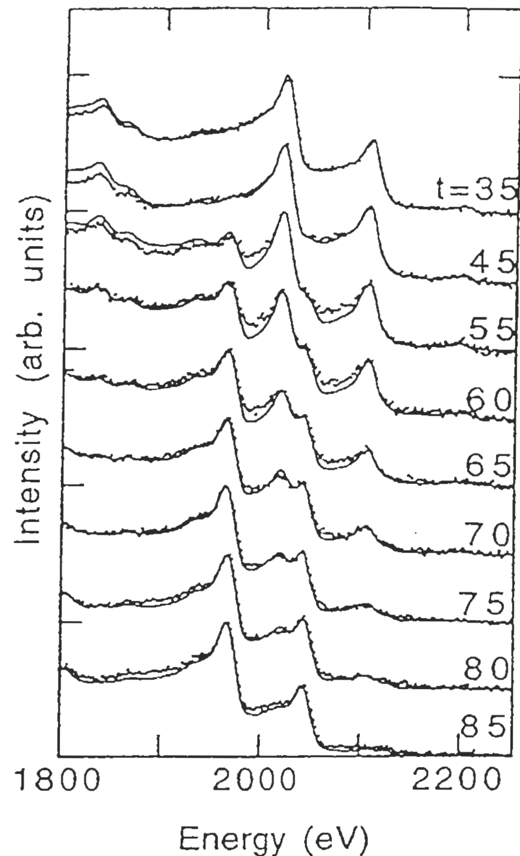

Fig. 7a Auger spectra of a Pt substrate covered with Au overlaers of different thickness (data points). Solid lines:theoretical spectra. The latter were calculated by first determining the depth profile from the raw measured data with a partial intensity analysis and subsequently applying Eq. (6).

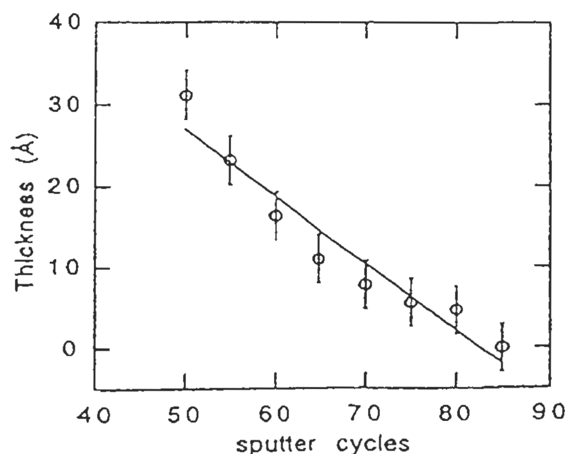

Fig. 7b Thickness of the Au overlayer for the different measurements shown in Fig. 7a. (see text).

that try to fit the data by theory. In such a case, improper analyzer transmission correction merely yields an incorrect profile without any means to assess an eventual error introduced in this way, while the partial intensity analysis provides an additional consistency check by a posteriori comparing the (calibrated) experimental data with the theoretical spectra.
As a final comment it is noted that the particular way to eliminate the background of inelastically backscattered primaries from the spectra shown in Fig. 7 is rather specific to the selected system of an Au overlayer on a Pt substrate and is not generally applicable. However, since we have seen that the partial intensity formalism is also able to accurately describe this background (see Fig. 5) as well as the Auger backscattering factor [40], the analysis of Auger spectra that includes the excitation mechanism of the signal electrons can be devised and is in fact presently being developed. Since a partial intensity analysis does not need very high resolution spectra (in fact the opposite is true: only the spectral intensity in ~10 channels is needed [11]) it should be possible to use data acquired on modern multichannel analyzers in combination with a scanning beam to perform true 3-dimensional nanostructure determination in this way.

6. Summary and Conclusions

Recent developments in the theoretical understanding of the signal generation in electron spectroscopy have been briefly reviewed. A general formalism describing the quantity assessable to experiment, i.e. the energy and angular distribution of signal electrons has been presented. This so–called partial intensity formalism can account for a sophisticated emission mechanism through the partial intensities, i.e. the number of electrons in the yield that have experienced a given number of inelastic collisions. It has been shown that the partial intensity formalism is able to account for a broad variety of phenomena in a simple manner. In particular, it is straightforward to incorporate the energy dependence of the scattering characteristics in the partial intensity formalism. From comparison of experimental as well as Monte Carlo model data with the results of the partial intensity formalism it may be concluded that this approach is accurate and effective.
Moreover, such a theoretical description quite naturally leads to a very general spectrum interpretation method, the so–called partial intensity analysis. This allows to derive the partial intensities from an experimental spectrum and to extract information on the concentrational depth profile while it also forms the basis for a general and consistent method to perform line shape analysis. A few examples of applications of a partial intensity analysis to model data as well as experimental Auger data have been given. Although these analyses demonstrate the potential of the method, a larger number of applications will have to be studied in order to fully explore its capabilities. One particularly attractive idea in this connection, that is presently being investigated, is application to multichannel scanning Auger data to perform non–destructive 3-D nanoanalysis.

References

1. A. Jablonski, Surf. Interf. Anal. 14 (1989) 659
2. I.S. Tilinin and W.S.M.Werner, Surf. Sci. 290(1993)119
3. V.M.Dwyer and J.A.D. Matthew, Surf. Sci. 143(1984)57
4. S. Tougaard, P. Sigmund, Phys. Rev. B25(1982)4452
5. P.L.J. Gunter and J.W. Niemantsverdriet, Applied Surf. Sci. 89(1995)69
6. W.S.M. Werner, Surf, Interf. Anal., 23(1995)696
7. C.J. Tung, Y.F. Chen, C. M. Kwei and T.L. Chou, Phys. Rev. B49(1994)16684
8. F. Yubero and S. Tougaard, Phys. Rev. B46(1992)2486
9. W.S.M.Werner, Phys. Rev. B52(1995)2964
10. I.S. Tilinin, A. Jablonski and S. Tougaard, Phys. Rev. B52(1995)5935
11. W.S.M. Werner, Surf. Interf. Anal. 23(1995)737
12. W.S.M. Werner, Phys. Rev. B, in print
13. S. Tanuma, C.J. Powell and D.R. Penn, Surf. Interf. Anal. 11(1988)577
14. C. J. Tung, J. C. Ashley and and R.H. Ritchie, Surf. Sci. 79(1981)427
15. D.R. Penn, Phys. Rev. B35(1985)482
16. W. Dolinski, S. Mroz and M. Zagorski, Surf. Sci. 200(1989)361
17. H. Beilschmidt, I.S. Tilinin and W.S.M.Werner, Surf. Interf. Anal. 22(1994)120
18. Y.F.Chen and C.M.Kwei and C.J.Tung, .

Phys.D.:Appl.Phys. 25(1992)262
19. C.J. Powell and M.P. Seah, J. Vac. Sci. Technol. 8(1990)735
20. M. P. Seah and G.C. Smith, Surf. Interf. Anal. 14(1989)823
21. M. P. Seah and G.C. Smith, Surf. Interf. Anal. 15(1990)751
22. M. P. Seah and G.C. Smith, Surf. Interf. Anal. 17(1990)855
23. H.H. Madden and J.E. Houston, J. Appl. Phys. 47(1976)307
24. P. Staib and J. Kirschner, Appl. Phys.3(1974)421
25. D.A. Shirley, Phys. Rev. B5 (1972)4709
26. J.T. Grant, T.W. Haas and J.E.Houston, Phys. Letters 45A(1973)309
27. D. Briggs and M. P. Seah (eds.) Practical Surface Analysis,Wiley,Chichester, 1983
28. T.P.Bussing and P.H.Holloway, J. Vac. Sci. Technol. A3(1985)1973
29. J.Tyler, D.G. Castner and B.D.Ratner, Surf. Interf. Anal. 14(1989)443
30. P. Cumpson, J. Electron Spect. Rel. Phen. 73(1995)25
31. S. Tougaard and H.S. Hansen, Surf. Interf. Anal. 14(1989)730
32. S. Tougaard, Surf. Interf. Anal. 8(1986)257
33. W.S.M.Werner, I.S. Tilinin, H. Beilschmid and M. Hayek, Surf. Interf. Anal. 21(1994)537
34. I.S. Tilinin,A. Jablonski and W.S.M. Werner, Prog. Surf. Sci. 52(1996)193
35. S. Tougaard, Surf. Interf. Anal. 11(1988)453
36. L. Landau, J. Phys. (*Moscow*) 8(1944)201
37. Z.-J Ding, T. Nagatomi, R. Shimizu and K. Goto, Surf. Sci. 336(1995)397
38. W.S.M. Werner, J. Vac. Sci. Technol., in print. (1997)
39. H. Wagner, C. Schiebl and W.S.M.Werner, Microchim. Acta 13(1996)623
40. H. Wagner and W.S.M.Werner, to be published